



**HAL**  
open science

## $H^\infty$ /LPV control for an active anti-roll bar system to improve the roll stability of heavy vehicles

van Tan Vu, Olivier Sename, Luc Dugard, van Phong Dinh, Thanh Phong Pham

► **To cite this version:**

van Tan Vu, Olivier Sename, Luc Dugard, van Phong Dinh, Thanh Phong Pham.  $H^\infty$  /LPV control for an active anti-roll bar system to improve the roll stability of heavy vehicles. 10th National Conference on Mechanics and the 8th National Congress of the Vietnam Association for Mechanics, Dec 2017, Hanoi, Vietnam. hal-01658083

**HAL Id: hal-01658083**

**<https://hal.science/hal-01658083>**

Submitted on 7 Dec 2017

**HAL** is a multi-disciplinary open access archive for the deposit and dissemination of scientific research documents, whether they are published or not. The documents may come from teaching and research institutions in France or abroad, or from public or private research centers.

L'archive ouverte pluridisciplinaire **HAL**, est destinée au dépôt et à la diffusion de documents scientifiques de niveau recherche, publiés ou non, émanant des établissements d'enseignement et de recherche français ou étrangers, des laboratoires publics ou privés.

# $H_\infty$ /LPV control for an active anti-roll bar system to improve the roll stability of heavy vehicles

Van Tan Vu<sup>a,c</sup>, Olivier Sename<sup>a</sup>, Luc Dugard<sup>a</sup>, Van Phong Dinh<sup>b</sup>, Thanh Phong Pham<sup>a</sup>

<sup>a</sup>Univ. Grenoble Alpes, CNRS, Grenoble INP\*, GIPSA-lab, 38000 Grenoble, France. E-mail: {Van-Tan.Vu, olivier.sename, luc.dugard, Thanh-Phong.Pham2}@gipsa-lab.grenoble-inp.fr

<sup>b</sup>Department of Applied Mechanics, SME, Hanoi University of Technology, Hanoi, Vietnam. E-mail: phong.dinhvan@hust.edu.vn

<sup>c</sup>Department of Automotive Mechanical Engineering, University of Transport and Communications, Hanoi, Vietnam

## Abstract:

Rollover accidents of heavy vehicles are especially dangerous and cause greater damage and injury than other accidents. The relatively low roll stability of heavy vehicles is the main cause of rollover and contributes to the total number of vehicle accidents. Most modern heavy vehicles are equipped with passive anti-roll bars, in order to enhance the roll stability. However, during cornering maneuvers, the passive anti-roll bar transfers the vertical forces of one side of the suspension to the other one, creating therefore a moment against the lateral force, so there may not be sufficient stability to overcome critical situations. This paper is focussed on the  $H_\infty$ /LPV active anti-roll bar control for single unit heavy vehicles. A Linear Parameter Varying (LPV) approach is proposed here in order to schedule the controller with the vehicle forward velocity as the varying parameter. The grid-based LPV approach is used to synthesize the  $H_\infty$ /LPV controller through LPVTools<sup>TM</sup>. The simulation results, both in the frequency and time domains, show that the  $H_\infty$ /LPV active anti-roll bar can improve the roll stability of the vehicle by 30%, when compared with the passive anti-roll bars.

**Keywords:** Vehicle dynamics, Heavy vehicle, Active anti-roll bar control, Linear Parameter Varying (LPV) control,  $H_\infty$  control, Roll stability.

## 1. INTRODUCTION

The role of heavy vehicles in economic development is very important. However, due to their high mass, there are also severe consequences for other road users when they are involved in accidents. The accidents related to heavy vehicles are also a complex issue, not only in developing countries, but also in developed countries like the USA and Europe. The rollover phenomenon is the most dangerous type of accident for heavy vehicles, and although rollovers are relatively rare events, they can be deadly when they occur. Loss of roll stability is the main cause of rollover accidents in which heavy vehicles are involved. According to the Federal National Highway Traffic Safety Administration (NHTSA), in the United States, there were 333.000 heavy vehicles involved in traffic crashes during 2012. There were 3.921 people killed in rollover crashes and 104.000 people injured (an increase of 18% from 2011). In 2013, more than 4.500 persons were killed in road traffic accidents involving heavy vehicles in the EU, constituting almost 18% of all road accident fatalities for that year [4]. While heavy vehicles account for just a small proportion of the vehicle fleet on the total vehicle kilometers travelled in the EU, they are more involved in severe road accidents, creating a significant need for a better understanding of the characteristics specific to this vehicle group.

---

\* Institute of Engineering Univ. Grenoble Alpes

In order to improve roll stability, most modern heavy vehicles are equipped with passive anti-roll bars to reduce roll motion. The advantage of the passive anti-roll bar is to reduce the body roll acceleration and roll angle during single wheel lifting and cornering maneuvers. However, the passive anti-roll bar also has drawbacks. During cornering maneuvers, it transfers the vertical forces of one side of the suspension to the other one, creating therefore a moment against the lateral force [15]. In order to overcome the drawbacks of the passive anti-roll bar systems, several schemes with possible active intervention into the vehicle dynamics have been proposed. One of them, the active anti-roll bars system uses a pair of hydraulic actuators that generate a stabilizing moment to counterbalance the overturning moment.

Besides, Linear Parameter Varying (LPV) systems are also an important class of systems, whose dynamics depend linearly on the state and input of the system, but could depend in a nonlinear way on scheduling parameters. The LPV paradigm considers that no *a priori* information about the scheduling parameter values is available, but that the parameter can be measured or estimated online [7], [8]. The interest in LPV systems is motivated by their use in gain-scheduling control techniques and by the possibility to embed nonlinear systems into the LPV framework by covering nonlinearities within the scheduling parameters. Therefore, the LPV framework enables, to some extent, the application of linear control methods to nonlinear systems, while providing strong supportive statements on stability and performance of the closed-loop system.

In [13] and [14], the authors used the  $H_\infty$  control method for the yaw-roll model of a single unit heavy vehicle. By using  $\mu$ -analysis, it is shown that the  $H_\infty$  active anti-roll bar control is robust w.r.t. the forward velocity and sprung mass variations. The simulation results in frequency and time domains show that the  $H_\infty$  active anti-roll bar control drastically reduces the normalized load transfer, compared to the passive anti-roll bar. One proves also that the efficiency of Genetic Algorithms that simplify the controller design to satisfy some performance objectives.

Based on the proposed  $H_\infty$  active anti-roll bar control system given in [13] and [14], this paper proposes an  $H_\infty$ /LPV controller that uses the forward velocity as the varying parameter. We extend latter works here, providing two new main contributions:

- The grid-based LPV approach [5] is used to synthesize the  $H_\infty$ /LPV controller depending on the forward velocity, through LPVTools<sup>TM</sup>. The normalized load transfers, the lateral acceleration and the limitations of the torque generated by actuators are taken into account.
- The simulation results, both in the frequency and time domains, prove the effectiveness of the  $H_\infty$ /LPV active anti-roll bar controller synthesis. This realistic solution drastically improves the roll stability of a single unit heavy vehicle, when compared to the results of the passive anti-roll bar.

The paper is organised as follows: Section 2 presents an LPV model of a single unit heavy vehicle. Section 3 gives the formulation of the  $H_\infty$ /LPV control problem. Section 4 illustrates the solution for the  $H_\infty$ /LPV control problem. Section 5 presents the simulation results in the frequency and time domains. Finally, some conclusions are drawn in section 6.

## 2. VEHICLE MODELLING: AN LPV APPROACH

The linear yaw-roll model of a single unit heavy vehicle is shown in Figure 1, with a three-body system, where  $m_s$  is the sprung mass,  $m_{uf}$  the unsprung mass at the front including the front wheels and axle, and  $m_{ur}$  the unsprung mass at the rear with the rear wheels and axle. The model

symbols are given in Table (1) and the parameters in [11]. The differential equations of the yaw-roll model that includes the lateral dynamics, the yaw moment, the roll moment of the sprung mass, the roll moment of the front and the rear unsprung masses, are formalized in the equations (1).

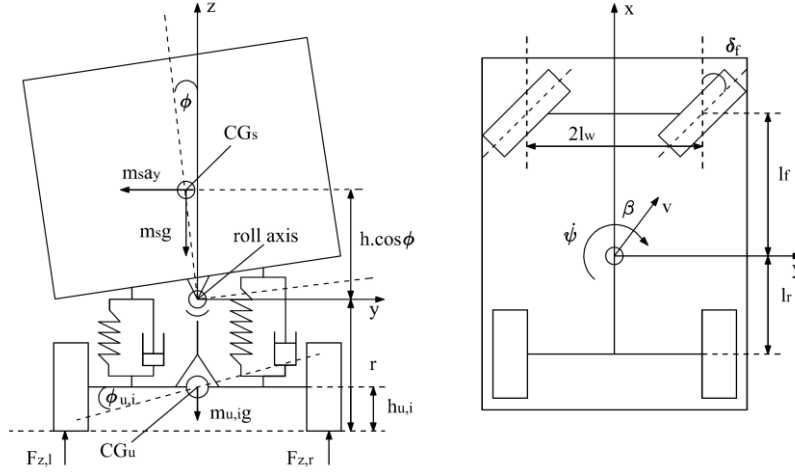


Figure 1: Yaw-Roll model of single unit heavy vehicle [11].

Table 1: Variables of yaw-roll model [11].

Symbols	Description	Symbols	Description
$m_s$	Sprung mass	$\delta_f$	Steering angle
$m_{u,f}$	Unsprung mass on the front axle	$C_f$	Tyre cornering stiffness on the front axle
$m_{u,r}$	Unsprung mass on the rear axle	$C_r$	Tyre cornering stiffness on the rear axle
$m$	The total vehicle mass	$k_f$	Suspension roll stiffness on the front axle
$v$	Forward velocity	$k_r$	Suspension roll stiffness on the rear axle
$v_{wi}$	Components of the forward velocity	$b_f$	Suspension roll damping on the front axle
$h$	Height of CG of sprung mass from roll axis	$b_r$	Suspension roll damping on the rear axle
$h_{u,i}$	Height of CG of unsprung mass from ground	$k_{fj}$	Tyre roll stiffness on the front axle
$r$	Height of roll axis from ground	$k_{tr}$	Tyre roll stiffness on the rear axle
$a_y$	Lateral acceleration	$I_{xx}$	Roll moment of inertia of sprung mass
$\beta$	Side-slip angle at center of mass	$I_{xz}$	Yaw-roll product of inertial of sprung mass
$\psi$	Heading angle	$I_{zz}$	Yaw moment of inertia of sprung mass
$\dot{\psi}$	Yaw rate	$l_f$	Length of the front axle from the CG
$\alpha$	Side slip angle	$l_r$	Length of the rear axle from the CG
$\phi$	Sprung mass roll angle	$l_w$	Half of the vehicle width
$\phi_{u,i}$	Unsprung mass roll angle	$\mu$	Road adhesion coefficient

$$\left\{ \begin{array}{l}
 mv(\dot{\beta} + \dot{\psi}) - m_s h \ddot{\phi} = F_{yf} + F_{yr} \\
 -I_{xz} \ddot{\phi} + I_{zz} \ddot{\psi} = F_{yf} l_f - F_{yr} l_r \\
 (I_{xx} + m_s h^2) \ddot{\phi} - I_{xz} \ddot{\psi} = m_s g h \phi + m_s v h (\dot{\beta} + \dot{\psi}) - k_f (\phi - \phi_{uf}) - b_f (\dot{\phi} - \dot{\phi}_{uf}) + M_{ARf} + T_f \\
 \quad - k_r (\phi - \phi_{ur}) - b_r (\dot{\phi} - \dot{\phi}_{ur}) + M_{ARr} + T_r \\
 -r F_{yf} = m_{uf} v (r - h_{uf}) (\dot{\beta} + \dot{\psi}) + m_{uf} g h_{uf} \phi_{uf} - k_{fj} \phi_{uf} + k_f (\phi - \phi_{uf}) + b_f (\dot{\phi} - \dot{\phi}_{uf}) + M_{ARf} + T_f \\
 -r F_{yr} = m_{ur} v (r - h_{ur}) (\dot{\beta} + \dot{\psi}) - m_{ur} g h_{ur} \phi_{ur} - k_{tr} \phi_{ur} + k_r (\phi - \phi_{ur}) + b_r (\dot{\phi} - \dot{\phi}_{ur}) + M_{ARr} + T_r
 \end{array} \right. \quad (1)$$

where  $T_f$ ,  $T_r$  are the torques at the two axles;  $M_{ARf}$ ,  $M_{ARr}$  are the moments of the passive anti-roll bar, which impact the unsprung and sprung masses at the front and rear axles [12]. The lateral tyre forces  $F_{yf,r}$  in the direction of velocity at the wheel ground contact points are modelled by a linear stiffness as [11]:

$$F_{yf} = \mu C_f \left( -\beta + \delta_f - \frac{l_f \dot{\psi}}{v} \right); \quad F_{yr} = \mu C_r \left( -\beta + \frac{l_r \dot{\psi}}{v} \right) \quad (2)$$

From equations (1) and (2), we can see that the yaw-roll model depends in a nonlinear way on the forward velocity  $v$ . Moreover, when the vehicle moves, the forward velocity is one of the constantly changing parameters, which depends on the driver and the motion condition of the vehicle. Here, the forward velocity  $v$  is chosen as a scheduling parameter. Denoting  $\rho = v$ , the vehicle model can be written in a state-space representation as follows:

$$\dot{x} = A(\rho)x + B_1(\rho)w + B_2(\rho)u \quad (3)$$

with the state vector  $x = \left[ \beta \quad \dot{\psi} \quad \varphi \quad \dot{\varphi} \quad \varphi_{uf} \quad \varphi_{ur} \right]$ , the disturbance input (steering angle)  $w = \left[ \delta_f \right]$  and the control inputs  $u = \left[ T_f \quad T_r \right]$ .

The model (3) is referred to as a Linear Parameter Varying (LPV) model, whose state-space entries depend continuously on a time varying parameter vector  $\rho$ . One characteristic of the LPV system is that it must be linear in a pair formed by the state vector ( $x$ ) and the control input vector ( $u$ ). The matrices  $A(\rho)$ ,  $B_1(\rho)$  and  $B_2(\rho)$  are here nonlinear functions of the scheduling vector  $\rho$ .

### 3. FORMULATION OF THE $H_\infty$ /LPV CONTROL PROBLEM

#### 3.1. Performance criteria

The objective of the active anti-roll bar control system is to maximize roll stability of the vehicle. Usually, an imminent rollover is detected when the calculated normalized load transfer ( $R_{f,r}$ ) given in (4) takes on the limit of  $\pm 1$  [6].

$$R_f = \frac{\Delta F_{zf}}{F_{zaf}}, \quad R_r = \frac{\Delta F_{zr}}{F_{zar}} \quad (4)$$

where  $F_{zaf}$  is the total axle load at the front axle and  $F_{zar}$  at the rear axle.  $\Delta F_{zf}$  and  $\Delta F_{zr}$  are the lateral load transfers at the front and rear axles [11], respectively.

The normalized load transfer  $R = \pm 1$  corresponds to the largest possible load transfer. In that case, the inner wheel in the bend lifts off. While attempting to minimize the load transfers, it is also necessary to constrain the roll angles between the sprung and unsprung masses ( $\varphi - \varphi_{uf,r}$ ) so that they stay within the limits of the suspension travel ( $7-8deg$ ) [11].

#### 3.2. Performance specifications for the $H_\infty$ /LPV control design

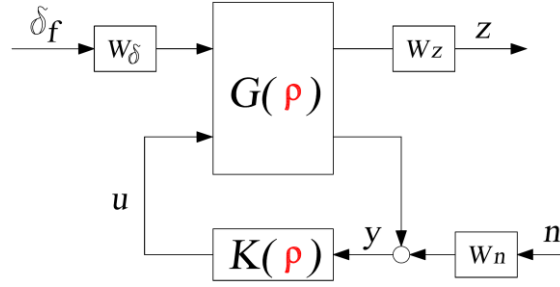


Figure 2: The closed-loop interconnection structure of the LPV active anti-roll bar control.

The closed-loop control scheme shown in Figure 2 is oriented towards control design. It includes the feedback structure of the nominal model  $G(\rho)$ , the controller  $K(\rho)$  and the weighting functions  $W_z$ ,  $W_\delta$ ,  $W_n$ . In this diagram,  $u$  is the control inputs,  $y$  the measured outputs,  $z$  the performance outputs,  $n$  is the measurement noises.  $\delta_f$ , set by the driver, is the steering angle considered as a disturbance signal.

The input scaling weight  $W_\delta$  normalizes the steering angle to the maximum expected command and is selected as  $W_\delta = \pi/180$ . This value corresponds to a  $1^\circ$  steering angle command. The weighting function  $W_n$  is selected as a diagonal matrix that accounts for sensor noise models in the control design. The noise weights are chosen as  $0.01$  ( $m/s^2$ ) for the lateral acceleration and  $0.01$  ( $^\circ/sec$ ) for the derivative of the roll angle  $\dot{\varphi}$  [11].

The weighting functions matrix  $W_z$  representing the performance output, is chosen as  $W_z = \text{diag}[W_{zTf}, W_{zTr}, W_{zRf}, W_{zRr}, W_{zay}]$ . The purpose of the weighting functions is to minimize the control inputs, normalized load transfers and the lateral acceleration over the desired frequency range. The weighting functions chosen for performance outputs can be considered as penalty functions, i.e., the weights should be large in the frequency range where small signals are desired and small where larger performance outputs can be tolerated.

The weighting functions  $W_{zTf}$  and  $W_{zTr}$  are chosen as  $W_{zTf} = 1/1.510^5$  and  $W_{zTr} = 1/210^5$ , which correspond to the front and rear control torques generated by the actuators.

The weighting functions  $W_{zRf}$  and  $W_{zRr}$  are selected as  $W_{zRf} = W_{zRr} = 1$ , which means that the maximal gain of the normalized load transfers can be 1 in the frequency domain for front and rear axles.

The weighting function  $W_{zay}$  is selected as:

$$W_{zay} = \frac{20}{100s + 0.01} \quad (5)$$

Indeed, the weighting function  $W_{zay}$  corresponds to a design that avoids the rollover situation with the bandwidth of the driver in the frequency range more than  $4$  rad/s. This weighting function will minimize directly the lateral acceleration when it reaches the critical value, and so avoid vehicle rollover.

### 3.3. The LPV generalized plant and $H_\infty$ /LPV control problem

According to Figure 2, the concatenation of the nonlinear model (3) with performance weighting functions has the following partitioned representation:

$$\begin{bmatrix} \dot{x}(t) \\ z(t) \\ y(t) \end{bmatrix} = \begin{bmatrix} A(\rho) & B_1(\rho) & B_2(\rho) \\ C_1(\rho) & D_{11}(\rho) & D_{12}(\rho) \\ C_2(\rho) & D_{21}(\rho) & D_{22}(\rho) \end{bmatrix} \begin{bmatrix} x(t) \\ w(t) \\ u(t) \end{bmatrix} \quad (6)$$

with the disturbance input  $w(t) = [\delta_f \ n]^T$ , the control input  $u(t) = [T_f \ T_r]^T$ , the performance output  $z(t) = [T_f, T_r, R_f, R_r, a_y]^T$  and the measured output  $y(t) = [a_y \ \dot{\varphi}]^T$ . It is worth noting that, in the LPV model of the active anti-roll bar system (6), the varying parameter  $\rho = v$  is known in real time and can be measured directly by sensors.

The control goal is to find a LPV controller  $K(\rho)$  defined as:

$$\begin{bmatrix} \dot{x}_k(t) \\ u(t) \end{bmatrix} = \begin{bmatrix} A_k(\rho) & B_k(\rho) \\ C_k(\rho) & D_k(\rho) \end{bmatrix} \begin{bmatrix} x_k(t) \\ y(t) \end{bmatrix} \quad (7)$$

where  $A_k(\rho)$ ,  $B_k(\rho)$ ,  $C_k(\rho)$ ,  $D_k(\rho)$  are continuous bounded matrix functions which minimize the induced  $L_2$  norm of the closed-loop LPV system  $\sum_{CL} = LFT(G, K)$ , with zero initial conditions, i.e.:

$$\|\sum_{CL}(\rho)\|_{2 \rightarrow 2} = \sup_{\substack{\rho \in P \\ \underline{v} \leq \dot{\rho} \leq \bar{v}}} \sup_{\substack{w \in L_2 \\ \|w\|_2 \neq 0}} \frac{\|z(\rho)\|_2}{\|w\|_2} \quad (8)$$

The existence of a controller that solves the parameter dependent LPV  $\gamma$ -performance problem can be expressed as the feasibility of a set of linear matrix inequalities (LMIs), which can be solved numerically [5], [10], [11].

#### 4. SOLUTION FOR THE $H_\infty$ /LPV CONTROL PROBLEM

According to the LPV generalized plant (6), several methods have arisen for representing the parameter dependence in LPV models, and then for designing the LPV controllers, such as: Linear Fractional Transformations (LFT) [2], Polytopic solution [3], Linearizations on a gridded domain (grid-based LPV) [5]. In this paper, the authors are interested in the grid-based LPV approach using the LPVTools<sup>TM</sup> toolbox [1], following the method developed by Wu [5].

##### 4.1. A solution to the LPV control design

The following theorem describes the LPV analysis problem when it is formulated in terms of the induced  $L_2$  norm of  $G(\rho)$  and the rate-bound  $(\bar{v}, \underline{v})$  of the parameter are taken into account [11].

**Theorem 1:** Given a compact set  $P \subset R^S$ , the performance level  $\gamma$  and the LPV system (7), with restriction  $D_{11}(\rho) = 0$ , the parameter-dependent  $\gamma$ -performance problem is solvable if there exist a continuously differentiable function  $X: R^S \rightarrow R^{n \times n}$  and  $Y: R^S \rightarrow R^{n \times n}$ , such that for all  $\rho \in P$ ,  $X(\rho) = X^T(\rho) > 0$ ,  $Y(\rho) = Y^T(\rho) > 0$  and

$$\begin{bmatrix} \hat{A}(\rho)X(\rho) + X(\rho)\hat{A}^T(\rho) - \sum_{i=1}^s (v_i \frac{\partial X}{\partial \rho_i}) - B_2(\rho)B_2^T(\rho) & X(\rho)C_1^T(\rho) & \gamma^{-1}B_1(\rho) \\ C_1(\rho)X(\rho) & -I_{ne} & 0 \\ \gamma^{-1}B_1^T(\rho) & 0 & -I_{nd} \end{bmatrix} < 0, \quad (9)$$

$$\begin{bmatrix} \tilde{A}^T(\rho)Y(\rho) + Y(\rho)\tilde{A}(\rho) + \sum_{i=1}^s (v_i \frac{\partial Y}{\partial \rho_i}) - C_2^T(\rho)C_2(\rho) & Y(\rho)B_1(\rho) & \gamma^{-1}C_1^T(\rho) \\ B_1^T(\rho)Y(\rho) & -I_{nd} & 0 \\ \gamma^{-1}C_1(\rho) & 0 & -I_{ne} \end{bmatrix} < 0, \quad (10)$$

$$\begin{bmatrix} X(\rho) & \gamma^{-1}I_n \\ \gamma^{-1}I_n & Y(\rho) \end{bmatrix} < 0 \quad (11)$$

where  $\hat{A}(\rho) = A(\rho) - B_2(\rho)C_1(\rho)$ ,  $\tilde{A}(\rho) = A(\rho) - B_1(\rho)C_2(\rho)$ . If these conditions are satisfied, the controller (7) exists and can solve the problem.

The constraints set by the LMIs in Theorem 1 are infinite dimensional, as is the solution space for  $\rho$ . The variables are  $X, Y: R^S \rightarrow R^{n \times m}$ , which restricts the search to the span of a collection of known scalar basis functions. By selecting the scalar continuous differentiable basis functions  $\{g_i: R^S \rightarrow R\}_{i=1}^{N_x}, \{f_i: R^S \rightarrow R\}_{i=1}^{N_y}$ , then the variables in Theorem 1 can be parametrized as:

$$X(\rho) = \sum_{i=1}^{N_x} g_i(\rho)X_i, Y(\rho) = \sum_{i=1}^{N_y} f_i(\rho)Y_i \quad (12)$$

Currently, there is no analytical method to select the basis functions, namely  $g_i$  and  $f_i$ . An intuitive rule for the basis function selection is to use those present in the open-loop state-space data. In our case, several power series  $\{1, \rho^2\}$  of the scheduling parameters are chosen, based on the lowest closed-loop  $L_2$  norm achieved.

#### 4.2. Grid-based LPV approach for the active anti-roll bar system

In this study, the grid-based LPV approach and LPVTools<sup>TM</sup> are used to synthesize the  $H_\infty$ /LPV active anti-roll bar control for heavy vehicles. It requires a gridded parameter space for the varying parameter  $\rho = v$ . In the interconnection structure, the spacing of the grid points is selected, based on how well the  $H_\infty$  point designs perform for plants around the design point. The  $H_\infty$  controllers are synthesized for 10 grid points of the forward velocity in the range  $\rho = v = [40 \div 130]$  km/h. The following commands are used to make the grid points as well as the LPV controller synthesis by using LPVTools<sup>TM</sup>: `rho = pgrid('rho', linspace(40/3.6, 130/3.6, 10))`. The weighting functions for both the performance and robustness specifications are considered unique for the whole grid. The effect of the proposed  $H_\infty$ /LPV active anti-roll bar controller to improve the roll stability of heavy vehicles will be explained in the next section.

### 5. SIMULATION RESULTS ANALYSIS

This section shows the simulation results, both in the frequency and time domains, to evaluate the effectiveness of the proposed  $H_\infty$ /LPV active anti-roll bar. The parameter values of the yaw-roll model are given in [11].



### 5.1. Analysis in the frequency domain

Rollover of the vehicle often occurs when the forward velocity is higher than 50 km/h. So, we only consider here the varying parameter  $\rho=v = [50 \text{ km/h}; 130 \text{ km/h}]$  with 9 grid points. Figure 3 shows respectively the transfer function magnitude of the normalized load transfers ( $R_{f,r}$ ) and the torques ( $T_{f,r}$ ) at the two axles.

As shown in Figure 3a,b, the  $H_\infty$ /LPV active anti-roll bar system reduces the normalized load transfers (at the two axles), compared to the passive anti-roll bar in the frequency range more than 4 rad/s, which represents the limited bandwidth of the driver [11]. Figure 3c,d shows the transfer function magnitude of the torques at the two axles. When the forward velocity increases, the torques generated by the actuators also increase. This indicates that the active anti-roll bar system requires more energy at higher forward velocities. However, the torques cannot increase too much, as they will exceed the saturation state of the actuators.

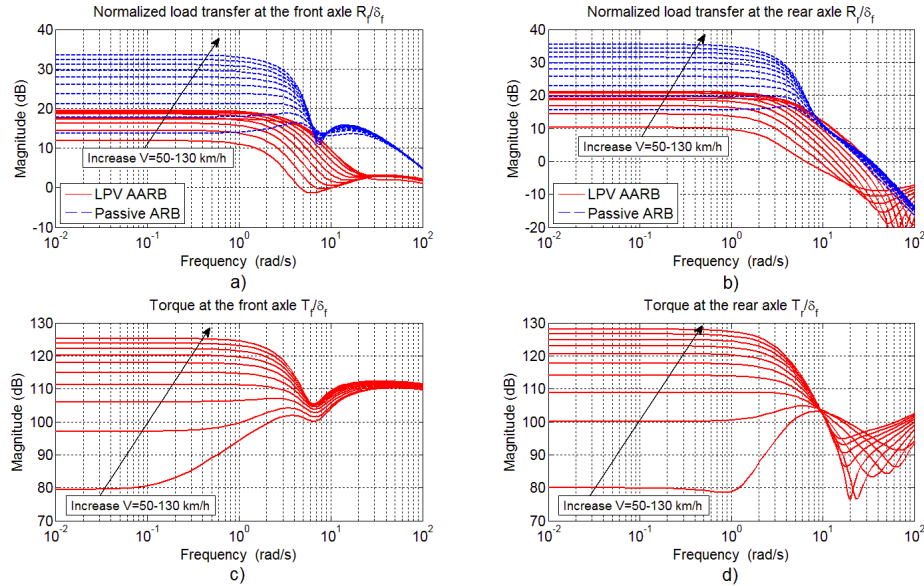


Figure 3: Transfer function magnitude of (a, b) the normalized load transfers, (c, d) the torques at the two axles.

### 5.2. Analysis in the time domain

In this section, a double lane change is used as the vehicle manoeuvre, a typical case to evaluate when avoiding an obstacle in an emergency. The manoeuvre has a 2.5m path deviation over 100m. The steering angle is shown in Figure 4a. The scenario used to validate the proposed  $H_\infty$ /LPV controller strategy for the active anti-roll bar system is the following:

- The initial forward velocity is 75 km/h, the vehicle runs on a dry road ( $\mu=1$ ). The total rolling resistance and aerodynamic resistance forces are ignored.
- When the obstacle is detected, the driver reduces the throttle and brakes to reduce the forward velocity of the vehicle. The total brake force increases from 0.5s to 1.5s and then the driver releases the brake pedal, as shown in Figure 4c.

The differential equation for the forward velocity in the case of the braking situation is determined as follows:

$$m\dot{v} = -\sum_{i=1}^4 F_{bi} \quad (13)$$

where  $F_{bi}$  is the brake force at each wheel. Due to the brake force, the forward velocity reduces from 75 km/h to 66.5 km/h, as in Figure 4b.

Figures 4d and 5a,b show the roll angle of the sprung mass and the normalized load transfers at both axles. In the passive anti-roll bar system case, the rollover actually occurs at the two axles simultaneously, but in the  $H_\infty/LPV$  active anti-roll bar control case, the normalized load transfers at the two axles are less than the limitation of  $\pm 1$ . The reduction of the normalized load transfers with the  $H_\infty/LPV$  active anti-roll bar is about 30%, when compared to the passive anti-roll bar. This indicates that the  $H_\infty/LPV$  active anti-roll bar control shows much improvement in roll stability when compared to the passive anti-roll bar. The torques at both axles are shown in Figure 5c,d. We can see that the maximum value of torque at the two axles are less than the limit of  $12 \cdot 10^4$  [Nm] [12].

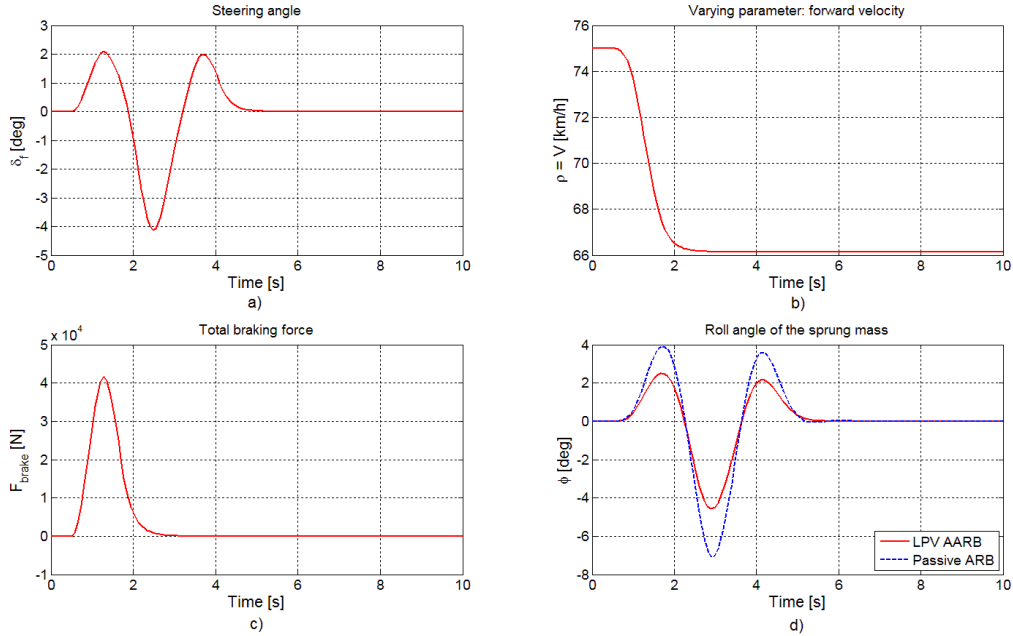


Figure 4: Time response of the steering angle, varying parameter, total braking force, roll angle of the sprung mass.

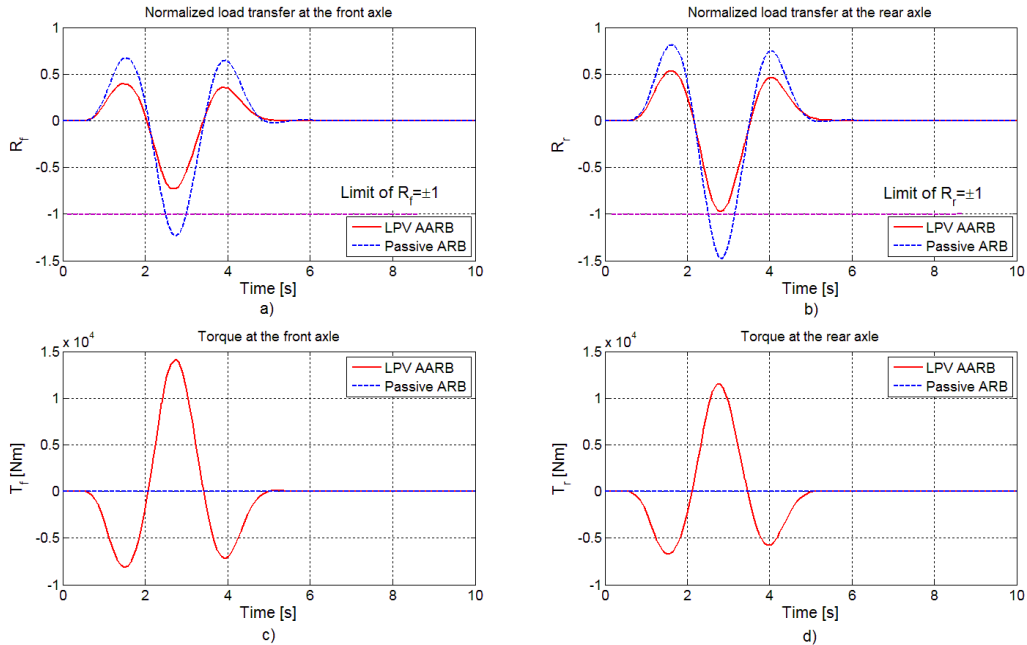


Figure 5: Time response of the normalized load transfers and torques at the two axles.

## 6. CONCLUSION

In this paper, the Yaw-Roll model of a single unit heavy vehicle including an active anti-roll bar system at both axles was used. An  $H_\infty/LPV$  control scheme with the forward velocity, considered as the varying parameter, is developed to maximize roll stability in order to prevent vehicle rollover. The normalized load transfers, the lateral acceleration and the limitations of the torque generated by the actuators are taken into account.

The simulation results, both in the frequency and time domains, have proven the effectiveness of the  $H_\infty/LPV$  active anti-roll bar controller synthesis, when compared to the results of the passive anti-roll bar.

Even if an  $H_\infty/LPV$  controller (scheduled by the vehicle velocity) seems to perform reasonably well here, the  $H_\infty/LPV$  controller with the adaptive weighting functions will also be of further interest.

## REFERENCES

- [1] A. Hjartarson, P. Seiler, A. Packard; *LPVtools: A toolbox for modeling, analysis, and synthesis of parameter varying control systems*; First IFAC Workshop on Linear Parameter Varying Systems; France (2015).
- [2] A. Packard; *Gain scheduling via linear fractional transformations*; Systems and Control Letters, 22(2), pp. 79-92 (1994).
- [3] C. Scherer, P. Gahinet, M. Chilali; *Multiobjective output feedback control via LMI optimization*; IEEE Transactions on Automatic Control, 42(7), pp. 896-911 (1997).
- [4] Evgenikos, Petros et al.; *Characteristics and Causes of Heavy Goods Vehicles and Buses Accidents in Europe*; Transportation Research Procedia, pp. 2158-2167 (2016).
- [5] F. Wu; *Control of linear parameter varying systems*; Ph.D. thesis, University of California at Berkeley; USA (1995).
- [6] Hsun-Hsuan, Huang, K.Yedavalli Rama, and A. Guenther Dennis; *Active roll control for rollover prevention of heavy articulated vehicles with multiple-rollover-index minimisation*; Vehicle System Dynamics; 50(3), pp. 471-493 (2012).
- [7] J. Mohammadpour, C. Scherer; *Control of Linear Parameter Varying Systems with Applications*; Springer (2012).
- [8] O. Sename, P. Gaspar, J. Bokor; *Robust Control and Linear Parameter Varying Approaches: Application to Vehicle Dynamics*; Springer (2013).
- [9] Sampson David and David Cebon; *Active Roll Control of Single Unit Heavy Road Vehicles*; Vehicle System Dynamics, 40(4), pp. 229-270 (2003).
- [10] P. Gaspar, J. Bokor, I. Szaszi; *Reconfigurable control structure to prevent the rollover of heavy vehicles*; Control Engineering Practice, 13 (6), pp. 699-711 (2005).
- [11] P. Gaspar, J. Bokor, I. Szaszi; *The design of a combined control structure to prevent the rollover of heavy vehicles*; European Journal of Control, 10(2), pp. 148–162 (2004).
- [12] V.T. Vu, O. Sename, P. Gaspar, L. Dugard, and P. Gaspar; *Enhancing roll stability of heavy vehicle by LQR active anti-roll bar control using electronic servo-valve hydraulic actuators*; Vehicle System Dynamics, 55(9), pp. 1405-1429 (2017).
- [13] V.T. Vu, O. Sename, P. Gaspar, L. Dugard, and P. Gaspar;  *$H_\infty$  active anti-roll bar control to prevent rollover of heavy vehicles: a robustness analysis*. IFAC Symposium on System Structure and Control - 6th SSSC; Istanbul, Turkey (2016).
- [14] V.T. Vu, O. Sename, P. Gaspar, L. Dugard, and P. Gaspar; *Optimal selection of weighting functions by genetic algorithms to design  $H_\infty$  anti-roll bar controllers for heavy vehicles*; Conference on vehicle system dynamics, identification and anomalies - 15th VSDIA; Budapest, Hungary (2016).
- [15] Zulkarnain, Noraishikin et al.; *Application of an Active Anti-roll Bar System for Enhancing Vehicle Ride and Handling*; IEEE Colloquium on Humanities, Science&Engineering Research; Sabah, Malaysia (2012).